Detecting long-term metabolic shifts using isotopomers: CO_2-driven suppression of photorespiration in C_3 plants over the 20th century

Ina Ehlers[a,1], Angela Augusti[a,1,2], Tatiana R. Betson[a], Mats B. Nilsson[b], John D. Marshall[b,c], and Jürgen Schleucher[a,3]

[a]Department of Medical Biochemistry & Biophysics, Umeå University, 901 87 Umea, Sweden; [b]Department of Forest Ecology and Management, Swedish University of Agricultural Sciences, 901 83 Umea, Sweden; and [c]Department of Forest, Rangeland, and Fire Sciences, University of Idaho, Moscow, ID 83844-1133

Edited by Katherine H. Freeman, Pennsylvania State University, University Park, PA, and approved November 9, 2015 (received for review July 26, 2015)

Terrestrial vegetation currently absorbs approximately a third of anthropogenic CO_2 emissions, mitigating the rise of atmospheric CO_2. However, terrestrial net primary production is highly sensitive to atmospheric CO_2 levels and associated climatic changes. In C_3 plants, which dominate terrestrial vegetation, net photosynthesis depends on the ratio between photorespiration and gross photosynthesis. This metabolic flux ratio depends strongly on CO_2 levels, but changes in this ratio over the past CO_2 rise have not been analyzed experimentally. Combining CO_2 manipulation experiments and deuterium NMR, we first establish that the intramolecular deuterium distribution (deuterium isotopomers) of photosynthetic C_3 glucose contains a signal of the photorespiration/photosynthesis ratio. By tracing this isotopomer signal in herbarium samples of natural C_3 vascular plant species, crops, and a *Sphagnum* moss species, we detect a consistent reduction in the photorespiration/photosynthesis ratio in response to the ∼100-ppm CO_2 increase between ∼1900 and 2013. No difference was detected in the isotopomer trends between beet sugar samples covering the 20th century and CO_2 manipulation experiments, suggesting that photosynthetic metabolism in sugar beet has not acclimated to increasing CO_2 over >100 y. This provides observational evidence that the reduction of the photorespiration/photosynthesis ratio was *ca.* 25%. The *Sphagnum* results are consistent with the observed positive correlations between peat accumulation rates and photosynthetic rates over the Northern Hemisphere. Our results establish that isotopomers of plant archives contain metabolic information covering centuries. Our data provide direct quantitative information on the "CO_2 fertilization" effect over decades, thus addressing a major uncertainty in Earth system models.

isotopomer | acclimation | deuterium | CO_2 fertilization | atmospheric change

Atmospheric CO_2 levels have increased from ∼200 ppm during the last ice age to currently 400 ppm, and they may, according to pessimistic scenarios, exceed 1,000 ppm in the year 2100 (1). Understanding plant responses to increasing CO_2 is currently hampered by two fundamental limitations: First, it is unknown how well manipulation experiments represent responses to the gradual CO_2 increase over decades and centuries. In Free-Air CO_2 Enrichment (FACE) experiments, which most closely mimic natural conditions, increases in $[CO_2]$ generally increase plant growth, but this "CO_2 fertilization" effect often declines after a few years of enrichment (2). Such transient responses may be related to the step increases in $[CO_2]$ used in the experiments, their limited duration (2), or factors other than CO_2 becoming limiting (3). Second, in response to the $[CO_2]$ increase since industrialization, genetic (4) and phenotypic plant responses (5–7) have been observed. Although century-scale changes have been detected in carbon isotopes ($\delta^{13}C$) and attributed to $[CO_2]$, these responses are tied to differences in intercellular substrate concentrations that reflect several metabolic fluxes and diffusion processes (8). However, the responses do not measure the metabolic fluxes directly. The consequently poor constraint of the magnitude of the CO_2 fertilization effect over decadal to century time scales (1, 9) is a major source of uncertainty in parameterizations of Earth system models (1, 10) and crop productivity models (11, 12). Therefore, observational data are essential to enable global carbon models to provide reliable long-term predictions.

Plants that fix carbon by the C_3 photosynthetic pathway (C_3 plants) account for most (*ca.* 75%) global primary production and human food production (13). In C_3 plants, CO_2 initially reacts with D-ribulose-1,5-bisphosphate (RubP) catalyzed by the enzyme D-ribulose-1,5-bisphosphate carboxylase/oxygenase (Rubisco), but this enzyme also has a competing O_2 fixation activity (14). The resulting carboxylation and oxygenation processes create photosynthetic and photorespiratory metabolic fluxes (15), which, respectively, cause C gains and losses for plants (Fig. 1), and which, globally, are among the largest biogeochemical C fluxes (16). Thus, the balance between these metabolic fluxes is a major determinant of the net primary productivity of C_3 plants in response to increasing $[CO_2]$, and therefore is a major influence on the CO_2 sink strength of terrestrial vegetation, including the performance of C_3 crop plants.

Significance

Decadal-scale metabolic responses of plants to environmental changes, including the magnitude of the "CO_2 fertilization" effect, are a major knowledge gap in Earth system models, in agricultural models, and for societal adaptation. We introduce intramolecular isotope distributions (isotopomers) as a methodology for detecting shifts in plant carbon metabolism over long times. Trends in a deuterium isotopomer ratio allow quantification of a biogeochemically relevant shift in the metabolism of C_3 plants toward photosynthesis, driven by increasing atmospheric CO_2 since industrialization. Isotopomers strongly increase the information content of isotope archives, and may therefore reveal long-term acclimation or adaptations to environmental changes in general. The metabolic information encoded in isotopomers of plant archives bridges a fundamental gap between experimental plant science and paleoenvironmental studies.

Author contributions: I.E., A.A., and J.S. designed research; I.E., A.A., and J.S. performed research; T.R.B. and M.B.N. contributed new reagents/analytic tools; I.E., A.A., T.R.B., M.B.N., J.D.M., and J.S. analyzed data; and I.E., A.A., T.R.B., M.B.N., J.D.M., and J.S. wrote the paper.

The authors declare no conflict of interest.

This article is a PNAS Direct Submission.

Freely available online through the PNAS open access option.

[1]I.E. and A.A. contributed equally to this work.

[2]Present address: Institute of Agro-environmental and Forest Biology, National Council of Research, 05010 Porano (TR), Italy.

[3]To whom correspondence should be addressed. Email: jurgen.schleucher@chem.umu.se.

This article contains supporting information online at www.pnas.org/lookup/suppl/doi:10.1073/pnas.1504493112/-/DCSupplemental.

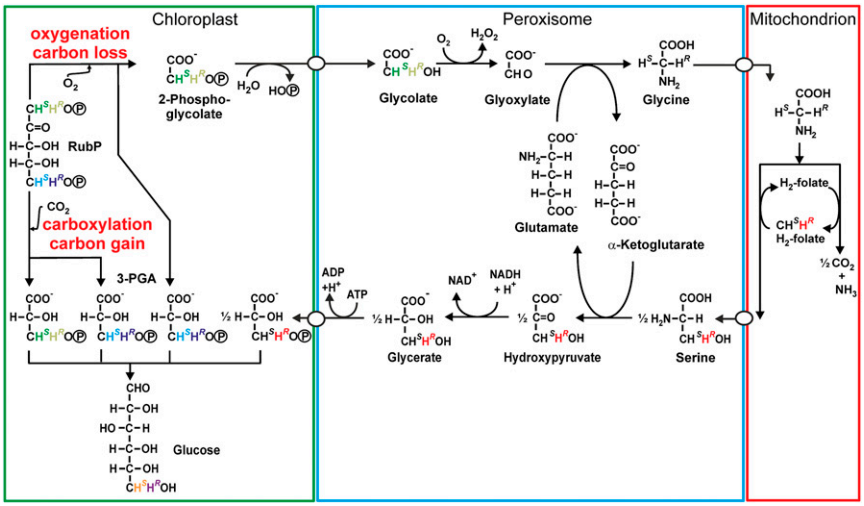

Fig. 1. Overview of metabolic pathways emanating from RubP by Rubisco activity. Upon carboxylation, 3-phosphoglycerate (3-PGA) molecules are formed from C1–C2 and C3–C5 of RuBP. Upon oxygenation, one 3-PGA molecule is formed from C3–C5 of RubP, and up to one-half 3-PGA is formed via the photorespiration pathway through the peroxisome and mitochondrion. The color coding of hydrogen atoms tracks the biochemical origins of hydrogens at C3 of 3-PGA, which give rise to the isotopomer signal encoded in the colored $C6H_2$ group of glucose.

Stable isotopes such as deuterium (D) are key tools for probing plants' ecological and biogeochemical interactions with their environment. Conventional compound-specific stable isotope methods provide the D/H ratio, usually expressed as δD (17), of an entire molecule, that is, averaged over all intramolecular positions in the molecule. This means that conventional stable isotope methods are based on isotopologues, which, by definition, differ in the number of isotopic substitutions. The same situation applies to the carbon isotope ratio $^{13}C/^{12}C$ expressed as $\delta^{13}C$. The δD or $\delta^{13}C$ signals of plant metabolites largely depend on three mechanisms: the isotope signatures of the plant's H_2O and CO_2 sources, isotope fractionation during substrate uptake, and isotope fractionation during biosynthesis, primarily enzyme isotope effects.

It is well established that enzyme isotope effects influence stable isotope abundance in specific intramolecular positions (18, 19). A molecule carrying an isotope substitution in a specific intramolecular position is termed an isotopomer. Deuterium isotopomer abundances can be measured by NMR. Glucose, measured as a derivative that gives highly resolved deuterium NMR spectra (see *Methods*), gives rise to seven signals with variable integrals (Fig. 2*A*), which reflect the abundance of each of the seven D isotopomers of glucose. Isotopomer variation encodes metabolic information (18, 19), but isotopomers have not yet been used for unraveling long-term metabolic changes induced by environmental drivers.

Here, we establish isotopomers as a ground-breaking technique for evaluating long-term effects of gradual $[CO_2]$ increase on plant metabolism at the biochemical level. We first use CO_2 manipulation experiments to identify an isotopomer signal that reflects the Rubisco oxygenation/carboxylation ratio of C_3 plants. We then trace the signal in herbarium samples of wild plants, crops, and *Sphagnum* mosses, to estimate changes in metabolic flux ratios in photosynthetic carbon metabolism of C_3 plants over the past century.

Results

An Isotopomer Signal of the Photorespiration/Photosynthesis Ratio. We first exposed sunflower (*Helianthus annuus*), a C_3 plant, to CO_2 concentrations ranging from 180 ppm to 1,500 ppm. Expansions of deuterium NMR spectra of a glucose derivative (Fig. 2*B*) show signals that reflect the abundances of the D isotopomers of the $C6H_2$ group of glucose; these hydrogens are stereochemically and biochemically distinct, which is indicated by the labeling as $D6^S$ and $D6^R$. The integral ratio of the signals, the $D6^S/D6^R$ ratio, differs

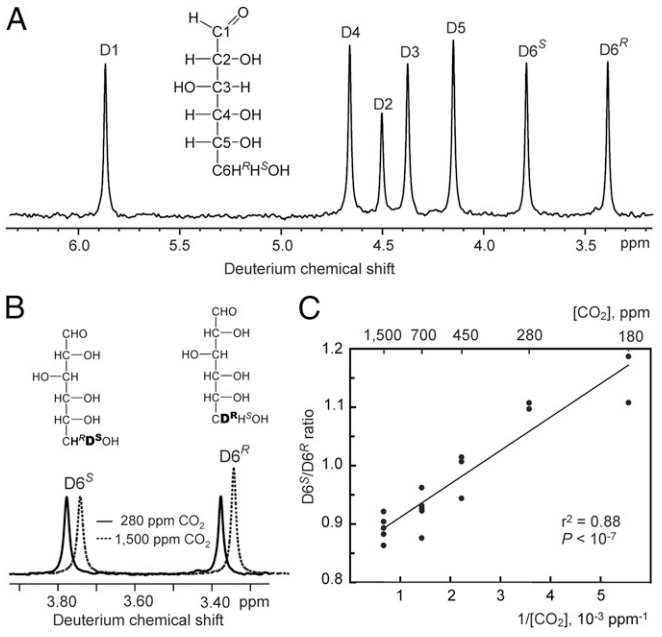

Fig. 2. Effect of $[CO_2]$ on the $D6^S/D6^R$ isotopomer ratio of photosynthetically generated glucose moieties in sunflower (*H. annuus*). (*A*) Deuterium NMR spectrum of a glucose derivative displaying one signal for each of the seven isotopomers of glucose. The signals' integrals are proportional to the isotopomer abundances. (*B*) Excerpts of deuterium NMR spectra of glucose prepared from sunflower leaf starch, showing signals arising from the $D6^S$ and $D6^R$ isotopomers of the $C6H_2$ group of glucose. The solid and dashed spectra were acquired from glucose formed at 280 ppm and 1,500 ppm CO_2, respectively. The dashed spectrum has been shifted sideways to ease comparison. (*C*) Dependence of the $D6^S/D6^R$ ratio of glucose from sunflower leaf starch on $1/[CO_2]$ (in units of 10^{-3} ppm^{-1}) during growth [$r^2 = 0.88$, slope 0.057 ±0.006 (SEM), $P < 10^{-7}$, $n = 17$, individual plants except for 180 and 280 ppm, where material from two to four plants had to be pooled for each sample].

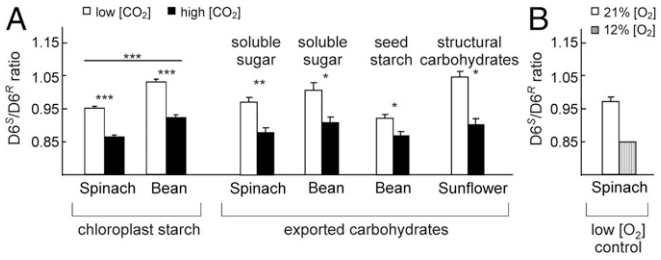

Fig. 3. Response of the $D6^S/D6^R$ ratio of different species and metabolites to manipulation of the $[CO_2]/[O_2]$ ratio. (*A*) $[CO_2]$ manipulation; white bars represent low and black bars represent high $[CO_2]$ of 360 ppm and 700 ppm, respectively, except for sunflower (200 ppm and 1,000 ppm). (*B*) O_2 manipulation; white bar represents ambient atmosphere, and gray bar represents ambient $[CO_2]$ with reduced $[O_2]$ (12%); glucose from soluble sugars was analyzed. Values are averages ± SEM (n = 2–5), except for one single sample pooled from several plants. *P < 0.05; **P < 0.01; ***P < 0.001 (ANOVA).

between the two spectra, which were obtained from glucose samples formed at 280 ppm and 1,500 ppm $[CO_2]$, respectively. When CO_2 is varied, the $D6^S/D6^R$ ratio shows a linear dependence on $1/CO_2$ (Fig. 2*C* and Table S1). Because sunflower is a C_3 plant, the oxygenation/carboxylation metabolic flux ratio at Rubisco is proportional to the concentration ratio of the competing substrates O_2/CO_2 (20, 21), which, at constant $[O_2]$, yields a linear dependence on $1/[CO_2]$. That the $D6^S/D6^R$ ratio reflects this metabolic flux ratio is supported by leaf gas exchange measurements (Fig. S1).

Photosynthetic oxygen production first appeared *ca.* 3 billion years ago, before which atmospheric $[O_2]$ was low (22). Since then, it has risen greatly, with a concomitant increase in the wasteful Rubisco oxygenation reaction. To cope with oxygenation, C_3 plants have evolved the photorespiration pathway to recycle oxygenation products (23). It appears that evolutionary changes could not suppress Rubisco's oxygenation activity, because of a strong trade-off between Rubisco's reaction rate and its CO_2/O_2 selectivity (8, 23–25). In contrast, C_4 plants largely suppress oxygenation by locally increasing $[CO_2]$ (23). Thus, $[CO_2]$ dependence of the $D6^S/D6^R$ ratio should be observable in all C_3 plants but should be absent in C_4 species. Accordingly, analysis of the $D6^S/D6^R$ ratio of chloroplast starch of two additional C_3 species grown at experimentally increased $[CO_2]$, spinach (*Spinacia oleracea*) and bean (*Phaseolus vulgaris*) (Fig. 3*A* and Table S2), confirmed the findings from sunflowers. In both species, the $D6^S/D6^R$ ratio decreased by ∼0.1 upon doubling $[CO_2]$, in accordance with the results from the experiment with sunflower (Fig. 2*C*). In marked contrast, but in agreement with the suppression of photorespiration in C_4 plants, the $D6^S/D6^R$ ratios of glucose formed under 450 ppm and 1,200 ppm in the C_4 species maize (*Zea mays*) were not significantly different (P = 0.9). Furthermore, reducing the O_2 concentration influenced the $D6^S/D6^R$ ratio in the same way as increasing $[CO_2]$ in the tested C_3 plants (Fig. 3*B*), as expected for suppression of photorespiration. These mechanistic tests lead us to conclude that the $D6^S/D6^R$ ratio is indeed a robust measure of the oxygenation/carboxylation metabolic flux ratio in C_3 plants.

Next, we tested if the $1/[CO_2]$ dependence of the $D6^S/D6^R$ ratio is preserved in glucose units of metabolites formed after export of carbohydrates from the chloroplast (leaf soluble sugars, leaf structural carbohydrates, and bean seed starch). The $D6^S/D6^R$ ratio in all metabolites depended on $[CO_2]$ as well (Fig. 3*A*), and statistical comparison of metabolites in bean and spinach revealed the same CO_2 response in leaf starch and soluble sugars, whereas, in bean seed starch, the response was smaller (two-way ANOVA, Table S2). This suggests that the $[CO_2]$ dependence of the $D6^S/D6^R$ ratio in initial photosynthates of C_3 plants may be weakened by subsequent metabolic transformations. A likely explanation is hydrogen isotope exchange with cellular water, which is known to occur during many enzyme reactions (26). If so, observed variations in the $D6^S/D6^R$ ratio would put lower bounds on the underlying change in the oxygenation/carboxylation ratio. Despite the exchange reactions, the data on exported metabolites show that physiological information encoded in the isotopomers is transmitted to long-lived metabolites.

CO_2 Increase Since Industrialization Has Shifted the Photorespiration/Photosynthesis Ratio. The $D6^S/D6^R$ ratio is sensitive to $[CO_2]$ across a concentration range including preindustrial to current levels (Fig. 2*C*). Therefore, analysis of the isotopomer ratio may retrospectively reveal metabolic shifts induced by increasing atmospheric $[CO_2]$. For a series of 18 archived sucrose samples from sugar beet, spanning the period 1890–2012 and a $[CO_2]$ increase from ∼295 ppm to ∼395 ppm, the $D6^S/D6^R$ ratio shows a highly significant linear dependence on $1/[CO_2]$ (Fig. 4 and Table S3). The regression slope (0.048 ± 0.012, SEM) is not significantly different from the slope determined for glucose moieties in greenhouse-grown sunflowers (Fig. 2*C*), showing that increasing atmospheric $[CO_2]$ has reduced the oxygenation/carboxylation ratio in sugar beet to the same degree as in our greenhouse manipulation experiments. The $[CO_2]$ dependence in archived beet sugar samples demonstrates that the photorespiration signal is highly robust, despite probable differences among the samples in agricultural practices, cultivars, and locations. This is remarkable, given that the modern samples and their progenitors experienced increasing $[CO_2]$ over more than 100 growing seasons. Furthermore, all modern plant breeding has occurred during this time period—after rediscovery of Mendel's laws in 1900—but has not detectably influenced the CO_2-driven change of the photosynthesis/photorespiration ratio. Finally, the agreement implies that the $[CO_2]$-driven metabolic shift during the past 100 y has not been counteracted by homeostatic adjustments of physiological properties, such as stomatal function or regulation of photosynthesis, in sugar beet.

The magnitude of CO_2 fertilization is a major uncertainty in models of the global carbon cycle and of crop productivity (1, 11). Assuming constant leaf and environmental properties,

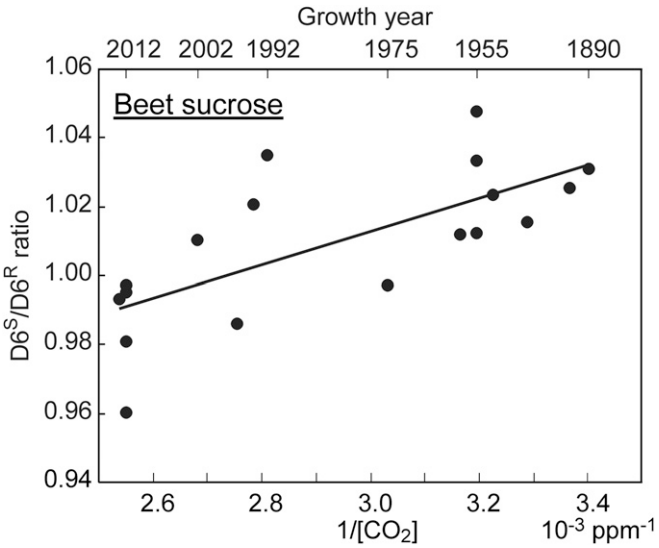

Fig. 4. Isotopomer response to changes in $[CO_2]$ in archived samples of beet sugar. $D6^S/D6^R$ ratios of the glucose moiety of beet sucrose samples as a function of $1/[CO_2]$ (in units of 10^{-3} ppm^{-1}) during the year of growth, shown on the upper x axis (r^2 = 0.49, P = 0.001, n = 18).

oxygenation/carboxylation ratios and net photosynthesis of C_3 plants can be modeled as a function of $[CO_2]$ using Rubisco kinetic parameters (21, 27). For the $[CO_2]$ increase from 295 ppm (~A.D. 1900) to 395 ppm (~A.D. 2012), such modeling predicts that the oxygenation/carboxylation ratio declined by ~25%, which contributed to an increase in net photosynthesis of about 35%. The agreement of the regression slopes obtained for our greenhouse-grown plants and the beet sugar samples indicates that this putative shift in metabolism has actually occurred in field-grown sugar beet between 1890 and 2012.

To further explore the generality of our observations, we compared herbarium and modern samples of an additional crop and two undomesticated C_3 species: the herbaceous crop spinach (*S. oleracea* L.), the vascular plant rosebay willowherb (or fireweed, *Epilobium angustifolium*), and a common peat moss species, *Sphagnum fuscum*. The modern samples of each species show significantly lower $D6^S/D6^R$ ratios, by 0.034–0.041, compared with the older herbarium samples (Fig. 5 and Table S3) that were produced at lower $[CO_2]$. This reduction is again consistent with a reduction in oxygenation due to the $[CO_2]$ increase during their respective growth periods. These results provide experimental evidence that the CO_2 increase since industrialization has shifted the photorespiration/photosynthesis ratio toward photosynthesis not only in crops grown under fertilized conditions but also in natural vegetation. *E. angustifolium* and *S. fuscum* both occur widely across the Northern Hemisphere. Because the underlying mechanism based on Rubisco properties is general for C_3 plants, these observations suggest that a substantial shift in the oxygenation/carboxylation ratio has occurred in terrestrial C_3 plants and it can be quantified using isotopomers.

Discussion

Origin of the Isotopomer Signal. We observed a dependence of the $D6^S/D6^R$ ratio on $1/[CO_2]$ in controlled experiments and in archival plant material. In the following, we explain this dependence by differences in isotope fractionation in the metabolic pathways originating from carboxylation and oxygenation, respectively, at Rubisco. The hydrogen atoms of the $C6H_2$ group of glucose can be traced back to their origins after carboxylation or oxygenation of ribulose bisphosphate (RuBP) in C_3 metabolism, as shown in Fig. 1. Although photorespiration leads to C loss, 3-phosphoglycerate (3-PGA) is formed after both carboxylation and oxygenation, but with differing stoichiometries and along differing paths. Numerous observations have shown that synthesis of a compound via different pathways induces different isotopomer distributions (18, 19, 28–32). No exception to this rule has been observed, and it agrees with the theory of isotope effects. Therefore, it is rational to assert that the PGA molecules formed from C3–C5 of RuBP, from C1–C2 of RuBP, and via the photorespiration pathway have differing D isotopomer ratios in their $C3H_2$ groups, as indicated by color coding in Fig. 1. In the photorespiration cycle, the $C3H_2$ group of 3-PGA originates from serine, which is formed by serine hydroxymethyl transferase. Commercial serine is produced by the same enzyme (33) and shows a strongly uneven isotopomer distribution in its $C3H_2$ group (Fig. S2). This supports the proposition that 3-PGA originating from photorespiration has a distinct isotopomer composition, and that serine hydroxymethyl transferase contributes to creation of the oxygenation/carboxylation signal. The ratio of metabolic fluxes originating from carboxylation and from oxygenation determines the contributions of the alternative PGA sources to the PGA pool, and the D isotopomer distribution of the PGA pool is a flux-weighted average of the PGA sources. During the conversion of PGA into glucose, no reaction occurs at the $C3H_2$ group; thus, there is no scrambling of hydrogen isotopes (34), and the D isotopomer ratio of the $C6H_2$ group of the resulting glucose will be identical to that of the PGA pool. Hence the weighted isotopomer distribution is transmitted from the 3-PGA pool to glucose, so that the $D6^S/D6^R$ ratio of glucose becomes dependent on the oxygenation/carboxylation ratio.

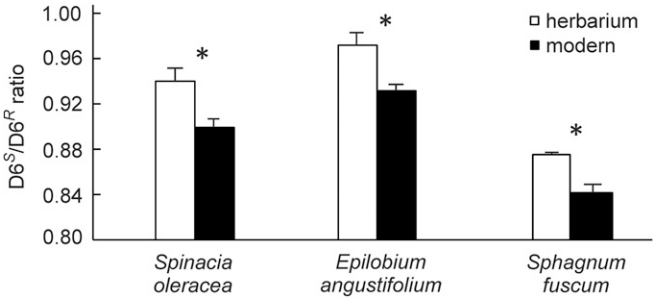

Fig. 5. Isotopomer response comparing herbarium and modern samples. $D6^S/D6^R$ ratios of structural carbohydrates of herbarium samples (open bars) and modern samples (black bars). Modern samples grew between 2011 and 2014, herbarium spinach samples grew between 1892 and 1908 ($[CO_2]$ ~295 ppm), herbarium *Epilobium* samples grew between 1943 and 1954 ($[CO_2]$ ~310 ppm), and herbarium *Sphagnum* samples grew between 1888 and 1923 ($[CO_2]$ ~295 ppm). Values are averages ± SEM (n = 3–6); *$P < 0.02$.

This dependence is the first example, to our knowledge, of an isotopomer shift induced by an environmental driver that can be mechanistically interpreted in terms of a metabolic response to this driver. We conclude that isotopomers carry metabolic signals that can be identified using laboratory experiments, and may be retrieved from archives of plant material.

Methodological Advantages of Isotopomer Signals. An important advantage of isotopomer ratios is that they can be interpreted without any reference to the δD of source water. This is possible because the δD of a plant's source and leaf water affect the abundance of all isotopomers to the same degree, so isotopomer ratios are independent of δD (35). Therefore, isotopomer ratios are exclusively determined by biochemical isotope effects. In contrast, interpretations of δD of plant archives are often complicated (36) because the required data on δD of source water and on evaporative enrichment of leaf water are not available. Because hydrogen isotope signatures are stable for $>10^4$ y (37), isotopomers may yield information on physiological changes on long time scales, including interglacial cycles. The complete D NMR spectrum of glucose (Fig. 2*A*) is fully described by seven isotopomer abundances, or by six isotopomer ratios and the overall amplitude of the spectrum, which is given by δD of the entire molecule. Thus, six out of seven degrees of freedom that describe the spectrum are isotopomer ratios, and hence the complete isotopomer pattern contains much more information than δD of the entire molecule.

Isotopomer information complements manipulation studies such as FACE experiments, in that information on metabolism can be retrieved on long time scales. Here we show that the primary metabolic response to elevated CO_2—suppression of photorespiration—has, in the species studied here, persisted during the 20th century. In contrast to the persistent suppression of photorespiration observed here, CO_2-driven increases in plant growth observed in FACE experiments often decline after a few years of CO_2 enrichment (2). Thus, combining FACE and isotopomer data may allow assessment of the role of factors besides photosynthesis that limit growth on the ecosystem level (38). Further studies will have to address whether long-term suppression of photorespiration has occurred for C3 plants in general, how photorespiration will develop under scenarios for future CO_2 levels and climate change, and how the global photorespiration flux will influence efforts to stabilize CO_2 levels.

Properties of Rubisco and the photorespiration cycle are current targets for crop improvement (20, 39). The $D6^S/D6^R$ ratio may be used to detect differences in CO_2 responses between crop species,

or cultivars, and isotopomers in general to monitor metabolic effects of crop engineering. Isotopomer variation exists for many other metabolites and isotopes, notably ^{13}C (40, 41). Therefore, time series of $\delta^{13}C$ of entire molecules may also be affected by isotopomer trends, and ^{13}C isotopomer analysis of plant archives can yield much more information than is available from $\delta^{13}C$.

Implications for Biogeochemistry and Plant Ecophysiology. Among the little that is known about responses of plants to increasing CO_2 over recent centuries, $\delta^{13}C$ time series of annual plant material or tree rings are arguably the strongest evidence. From $\delta^{13}C$, increases in assimilation have been deduced, and the reduction in the oxygenation/carboxylation ratio is a large part of this. Our isotopomer results provide the first empirical data on the magnitude of the shift in this central biogeochemical flux ratio.

Forests make a big contribution to the global carbon cycle, and tree rings are one of the most prominent paleoarchives. Therefore, it is important to note that isotopomer information may be retrieved from tree rings, because the glucose derivative can be produced from whole wood or cellulose (35). Furthermore, we have previously shown that metabolic signatures produced on the leaf level are preserved in the glucose moieties obtained from tree rings (42). This indicates that it will be possible to derive long-term physiological information from tree rings. Because glucose can sometimes be produced from fossil leaves, paleoatmospheric reconstruction of atmospheric CO_2 may also be possible.

The peat mosses belonging to the genus *Sphagnum* are the main constituents of peat of high-latitude mires (43, 44). This peat has accumulated during the Holocene and currently represents ∼25% of the global soil carbon pool. The amount of carbon stored in peat has caused a lowering of the contemporary atmospheric CO_2 concentration by 35 ppm (45). Due to the extraordinarily large carbon store in these peatlands, their feedback to changing climate and rising CO_2 constitutes a major scientific and societal concern with respect to predicting future biosphere–atmosphere CO_2 exchange and storage (44, 46). Recent studies have revealed net primary production as the main driver for peatland carbon accumulation (46, 47), which is also supported by the observation that incoming photosynthetic active radiation during the growing season is the main driver for geographic variation in *Sphagnum* moss productivity (48). The studied species *S. fuscum* grows in hummocks and is thus directly exposed to atmospheric CO_2. Such hummock-forming sphagnum species dominate peat formation at high-latitude mires (48). The trend in the isotopomer ratio observed in *S. fuscum* constitutes the first evidence of increased photosynthesis among peat-forming *Sphagnum* mosses in response to the century-scale CO_2 increase under natural conditions. Thus, by applying isotopomers to a geographic and species range of peat-forming species, it may be possible to assess general trends in the physiology of peat-forming species. Trends in net photosynthesis may then be scaled up to the global scale, to obtain a mechanistic understanding of the carbon balance of peatlands.

Reducing the photorespiration/photosynthesis ratio increases the light use efficiency of photosynthesis. Some measure of light use efficiency is frequently used to parameterize photosynthetic algorithms in models of ecosystem response to climate change (49–51). These parameterizations have been based on models of Rubisco substrate specificity (27) scaled up to the ecosystem level or, more often, empirical fitting from remote sensing (52), eddy covariance (53), or biomass (54) data that was scaled downward and thus lacked a mechanistic description of this key metabolic flux ratio. The isotopomer approach thus provides a mechanistically based means of parameterizing light use efficiency models, allowing us to improve our predictions. These improvements will appear in both paleoarchive data, looking backward, and the use of experimental CO_2 enrichment experiments, to look forward.

Information on effects of long-term increases in $[CO_2]$ on the metabolism of crops and natural vegetation is essential for understanding underlying mechanisms and robustly modeling C exchange fluxes between terrestrial vegetation and the atmosphere. The presented methodology may be used to detect variation in the CO_2 responses between species or crop lines, and changes in isotopomer patterns may be used to detect long-term acclimation or adaptation. Retrieving such information will enable the time frames of plant physiological studies to be extended to centuries, thereby bridging the gap between manipulation experiments and paleoenvironmental studies.

Methods

CO_2 Manipulation Experiments. In greenhouse and growth chamber experiments, *Helianthus annuus*, *Z. mays*, *S. oleracea*, and *P. vulgaris* plants were exposed to different atmospheric $[CO_2]$ levels, and *S. oleracea* was exposed to reduced $[O_2]$. Gas exchange parameters of *H. annuus* leaves were determined using a two-channel fast response measurement system (Fast-Est), described in detail in ref. 55. Details of growth and measurement conditions are provided in *Supporting Information*.

Historic Plant Material. Eighteen archived sugar beet sucrose samples that grew between 1890 and 2012 were obtained from sources listed in Table S3 (specified growth years of these samples are as stated by the contributors). Current samples (2011–2012) are dated to the previous growing season. Herbarium samples of *S. oleracea, E. angustifolium*, and *S. fuscum* were obtained from the herbarium at Umeå University and from Naturhistoriska Riksmuseet. Modern samples for comparison were either commercial frozen products (spinach) or were collected in Sweden. Exact origins, growth locations, and growth years are provided in Table S3. Structural carbohydrates were analyzed.

Sample Preparation for NMR Isotopomer Measurements. For deuterium NMR measurements, pure samples of a glucose derivative were prepared from all samples, as follows. Soluble sugars were extracted from leaf material according to previously used methods (35, 56), starting with 10 g of fresh material. Starch from chloroplasts was extracted from the pellet resulting from extraction of soluble sugars, according to ref. 57, with the following modifications: 200 mL of 50 mM KOH was added, and the solution was kept at 90 °C for 2 h. After cooling on ice, the pH was adjusted to 4.7 with 1 M acetic acid, and 42 units of amyloglucosidase (Roche) were added. After incubation at 37 °C overnight, samples were centrifuged for 20 min at 4,000 × *g*, and the supernatant was collected. Starch from bean fruits was hydrolyzed to glucose by amyloglucosidase treatment. Leaf structural carbohydrates were obtained by removing soluble sugars and starch from leaves by extraction and amyloglucosidase hydrolysis, respectively. Structural carbohydrates were hydrolyzed to glucose according to Betson et al. (35). Sugar samples prepared from plants were dried in vacuum and were converted into a pure glucose derivative suitable for deuterium NMR analysis (35).

Isotopomer Quantification. Deuterium NMR measurements and subsequent data analysis followed Schleucher et al. (19), modified as previously described (35). For NMR measurements, we used a DRX600 spectrometer (Bruker) equipped with a 5-mm broadband observe probe and a ^{19}F lock device, or an AVANCE III 850 spectrometer (Bruker) equipped with a cryogenic probe optimized for deuterium detection and equipped with a ^{19}F lock. Deuterium NMR spectra were integrated by deconvolution with a Lorentzian line shape fit, using TopSpin software (version 3.1; Bruker). The $D6^S/D6^R$ isotopomer ratio was determined as the ratio of the integrals of the $D6^S$ and $D6^R$ signals.

Statistical Analysis. For each sample, five or six replicate spectra were recorded, the average isotopomer ratio among the spectra was used, and its SE was calculated to estimate measurement precision. For biological replicate samples, SEs were calculated. The significance of between-treatment differences in isotopomer ratios was tested using ANOVA, and linear regression analysis was applied to test relationships between the ratios and $[CO_2]$ (in both cases using Excel).

ACKNOWLEDGMENTS. We thank the late Stefan Ericsson, Herbarium UME, Umeå University, for assistance with acquiring herbarium plant samples. We thank several institutions and colleagues for providing samples and for valuable advice on the manuscript, and Vaughan Hurry and Agu Laisk for help with the gas exchange measurements. This study was supported by the National Magnetic Resonance Facility at Madison, the Centre for Environmental Research in Umeå, the Swedish Research Council VR, the Kempe foundations, and the "NMR for Life" facility.

1. Intergovernmental Panel on Climate Change (2013) *Climate Change 2013: The Physical Science Basis. Contribution of Working Group I to the Fifth Assessment Report of the Intergovernmental Panel on Climate Change*, eds. Stocker TF, et al. (Cambridge Univ Press, Cambridge, UK).
2. Leuzinger S, et al. (2011) Do global change experiments overestimate impacts on terrestrial ecosystems? *Trends Ecol Evol* 26(5):236–241.
3. Drake JE, et al. (2011) Increases in the flux of carbon belowground stimulate nitrogen uptake and sustain the long-term enhancement of forest productivity under elevated CO_2. *Ecol Lett* 14(4):349–357.
4. Jump AS, Hunt JM, Martínez-Izquierdo JA, Peñuelas J (2006) Natural selection and climate change: Temperature-linked spatial and temporal trends in gene frequency in *Fagus sylvatica*. *Mol Ecol* 15(11):3469–3480.
5. Hetherington AM, Woodward FI (2003) The role of stomata in sensing and driving environmental change. *Nature* 424(6951):901–908.
6. Penuelas J, Canadell JG, Ogaya R (2011) Increased water-use efficiency during the 20th century did not translate into enhanced tree growth. *Glob Ecol Biogeogr* 20(4): 597–608.
7. Woodward FI (1987) Stomatal numbers are sensitive to increases in CO_2 from pre-industrial levels. *Nature* 327(6123):617–618.
8. Franks PJ, et al. (2013) Sensitivity of plants to changing atmospheric CO_2 concentration: From the geological past to the next century. *New Phytol* 197(4):1077–1094.
9. Leakey ADB, Lau JA (2012) Evolutionary context for understanding and manipulating plant responses to past, present and future atmospheric [CO_2]. *Philos Trans R Soc Lond B Biol Sci* 367(1588):613–629.
10. Le Quéré C, et al. (2009) Trends in the sources and sinks of carbon dioxide. *Nat Geosci* 2(12):831–836.
11. Long SP, Ainsworth EA, Leakey ADB, Nösberger J, Ort DR (2006) Food for thought: Lower-than-expected crop yield stimulation with rising CO_2 concentrations. *Science* 312(5782):1918–1921.
12. Lobell DB, Schlenker W, Costa-Roberts J (2011) Climate trends and global crop production since 1980. *Science* 333(6042):616–620.
13. Beer C, et al. (2010) Terrestrial gross carbon dioxide uptake: Global distribution and covariation with climate. *Science* 329(5993):834–838.
14. Ogren WL, Bowes G (1971) Ribulose diphosphate carboxylase regulates soybean photorespiration. *Nat New Biol* 230(13):159–160.
15. Laing WA, Ogren WL, Hageman RH (1974) Regulation of soybean net photosynthetic CO_2 fixation by interaction of CO_2, O_2, and ribulose 1,5-diphosphate carboxylase. *Plant Physiol* 54(5):678–685.
16. Beerling DJ, Woodward FI (2001) *Vegetation and the Terrestrial Carbon Cycle: Modelling the First 400 Million Years* (Cambridge Univ Press, Cambridge, UK).
17. Wolfsberg M, Van Hook WA, Paneth P, Rebelo LP (2010) *Isotope Effects in the Chemical, Geological, and Bio Sciences* (Springer, Heidelberg), pp 290–292.
18. Schmidt H-L (2003) Fundamentals and systematics of the non-statistical distributions of isotopes in natural compounds. *Naturwissenschaften* 90(12):537–552.
19. Schleucher J, Vanderveer P, Markley JL, Sharkey TD (1999) Intramolecular deuterium distributions reveal disequilibrium of chloroplast phosphoglucose isomerase. *Plant Cell Environ* 22(5):525–533.
20. Parry MAJ, et al. (2013) Rubisco activity and regulation as targets for crop improvement. *J Exp Bot* 64(3):717–730.
21. Sharkey TD (1988) Estimating the rate of photorespiration in leaves. *Physiol Plant* 73(1):147–152.
22. Tomitani A, Knoll AH, Cavanaugh CM, Ohno T (2006) The evolutionary diversification of cyanobacteria: Molecular–phylogenetic and paleontological perspectives. *Proc Natl Acad Sci USA* 103(14):5442–5447.
23. Foyer CH, Bloom AJ, Queval G, Noctor G (2009) Photorespiratory metabolism: Genes, mutants, energetics, and redox signaling. *Annu Rev Plant Biol* 60:455–484.
24. Fernie AR, et al. (2013) Perspectives on plant photorespiratory metabolism. *Plant Biol (Stuttg)* 15(4):748–753.
25. Tcherkez GGB, Farquhar GD, Andrews TJ (2006) Despite slow catalysis and confused substrate specificity, all ribulose bisphosphate carboxylases may be nearly perfectly optimized. *Proc Natl Acad Sci USA* 103(19):7246–7251.
26. Rose IA (1975) Mechanism of the aldose-ketose isomerase reactions. *Adv Enzymol Relat Areas Mol Biol* 43:491–517.
27. Farquhar GD, von Caemmerer S, Berry JA (1980) A biochemical model of photosynthetic CO_2 assimilation in leaves of C_3 species. *Planta* 149(1):78–90.
28. Zhang B-L, et al. (2002) Hydrogen isotopic profile in the characterization of sugars. Influence of the metabolic pathway. *J Agric Food Chem* 50(6):1574–1580.
29. Martin GJ, Martin ML, Zhang B-L (1992) Site-specific natural isotope fractionation of hydrogen in plant products studied by nuclear magnetic resonance. *Plant Cell Environ* 15(9):1037–1050.
30. Zhang B-L, Quemerais B, Martin ML, Martin GJ, Williams JM (1994) Determination of the natural deuterium distribution in glucose from plants having different photosynthetic pathways. *Phytochem Anal* 5(3):105–110.
31. Tenailleau EJ, Lancelin P, Robins RJ, Akoka S (2004) Authentication of the origin of vanillin using quantitative natural abundance ^{13}C NMR. *J Agric Food Chem* 52(26): 7782–7787.
32. Fronza G, et al. (2001) The positional $\delta(^{18}O)$ values of extracted and synthetic vanillin. *Helv Chim Acta* 84(2):351–359.
33. Elvers B, ed (2014) *Ullmann's Fine Chemicals* (Wiley-VCH, Weinheim, Germany), Vol 3.
34. Hanson KR (1984) Stereochemical determination of carbon partitioning between photosynthesis and photorespiration in C_3 plants: Use of $(3R)$-$_D$-[3-$^3H_1$, 3-^{14}C]glyceric acid. *Arch Biochem Biophys* 232(1):58–75.
35. Betson TR, Augusti A, Schleucher J (2006) Quantification of deuterium isotopomers of tree-ring cellulose using nuclear magnetic resonance. *Anal Chem* 78(24):8406–8411.
36. McCarroll D, Loader NJ (2004) Stable isotopes in tree rings. *Quat Sci Rev* 23(7-8): 771–801.
37. Sessions AL, Sylva SP, Summons RE, Hayes JM (2004) Isotopic exchange of carbon-bound hydrogen over geologic timescales. *Geochim Cosmochim Acta* 68(7): 1545–1559.
38. Norby RJ, Zak DR (2011) Ecological lessons from Free-Air CO_2 Enrichment (FACE) experiments. *Annu Rev Ecol Evol Syst* 42:181–203.
39. Nölke G, Houdelet M, Kreuzaler F, Peterhänsel C, Schillberg S (2014) The expression of a recombinant glycolate dehydrogenase polyprotein in potato (*Solanum tuberosum*) plastids strongly enhances photosynthesis and tuber yield. *Plant Biotechnol J* 12(6): 734–742.
40. Rossmann A, Butzenlechner M, Schmidt HL (1991) Evidence for a nonstatistical carbon isotope distribution in natural glucose. *Plant Physiol* 96(2):609–614.
41. Chaintreau A, et al. (2013) Site-specific ^{13}C content by quantitative isotopic ^{13}C nuclear magnetic resonance spectrometry: A pilot inter-laboratory study. *Anal Chim Acta* 788:108–113.
42. Augusti A, Betson TR, Schleucher J (2008) Deriving correlated climate and physiological signals from deuterium isotopomers in tree rings. *Chem Geol* 252(1-2):1–8.
43. Gorham E (1991) Northern peatlands: Role in the carbon cycle and probable responses to climatic warming. *Ecol Appl* 1(2):182–195.
44. Loisel J, et al. (2014) A database and synthesis of northern peatland soil properties and Holocene carbon and nitrogen accumulation. *Holocene* 24(9):1028–1042.
45. Frolking S, Roulet NT (2007) Holocene radiative forcing impact of northern peatland carbon accumulation and methane emissions. *Glob Change Biol* 13(5):1079–1088.
46. Charman DJ, et al. (2013) Climate-related changes in peatland carbon accumulation during the last millennium. *Biogeosciences* 10(2):929–944.
47. Lund M, et al. (2010) Variability in exchange of CO_2 across 12 northern peatland and tundra sites. *Glob Change Biol* 16(9):2436–2448.
48. Loisel J, Gallego-Sala AV, Yu Z (2012) Global-scale pattern of peatland *Sphagnum* growth driven by photosynthetically active radiation and growing season length. *Biogeosciences* 9(7):2737–2746.
49. Medlyn BE (1998) Physiological basis of the light use efficiency model. *Tree Physiol* 18(3):167–176.
50. Sitch S, et al. (2003) Evaluation of ecosystem dynamics, plant geography and terrestrial carbon cycling in the LPJ dynamic global vegetation model. *Glob Change Biol* 9(2):161–185.
51. Turner DP, et al. (2003) Scaling gross primary production (GPP) over boreal and deciduous forest landscapes in support of MODIS GPP product validation. *Remote Sens Environ* 88(3):256–270.
52. Hilker T, Coops NC, Wulder MA, Black TA, Guy RD (2008) The use of remote sensing in light use efficiency based models of gross primary production: A review of current status and future requirements. *Sci Total Environ* 404(2-3):411–423.
53. Yuan W, et al. (2007) Deriving a light use efficiency model from eddy covariance flux data for predicting daily gross primary production across biomes. *Agric For Meteorol* 143(3-4):189–207.
54. Landsberg JJ, Waring RH (1997) A generalised model of forest productivity using simplified concepts of radiation-use efficiency, carbon balance and partitioning. *For Ecol Manage* 95(3):209–228.
55. Laisk A, Edwards GE (1997) CO_2 and temperature-dependent induction in C4 photosynthesis: An approach to the hierarchy of rate-limiting processes. *Aust J Plant Physiol* 24(4):505–516.
56. Augusti A, Betson TR, Schleucher J (2006) Hydrogen exchange during cellulose synthesis distinguishes climatic and biochemical isotope fractionations in tree rings. *New Phytol* 172(3):490–499.
57. Hurry V, Strand A, Furbank R, Stitt M (2000) The role of inorganic phosphate in the development of freezing tolerance and the acclimatization of photosynthesis to low temperature is revealed by the pho mutants of *Arabidopsis thaliana*. *Plant J* 24(3): 383–396.
58. Lehmeier CA, Schäufele R, Schnyder H (2005) Allocation of reserve-derived and currently assimilated carbon and nitrogen in seedlings of *Helianthus annuus* under sub-ambient and elevated CO growth conditions. *New Phytol* 168(3):613–621.
59. Sumberg A (1995) Laisk A. *Photosynthesis: From Light to Biosphere*, ed Mathis P (Kluwer Acad, Dordrecht, The Netherlands), Vol 5, pp 615–618.
60. Laisk A, Sumberg A (1994) Partitioning of the leaf CO_2 exchange into components using CO_2 exchange and fluorescence measurements. *Plant Physiol* 106(2):689–695.
61. Tcherkez G (2013) Is the recovery of (photo) respiratory CO_2 and intermediates minimal? *New Phytol* 198(2):334–338.